Attenuation measurement uncertainties caused by speckle statistics

Kevin J. Parker
Department of Electrical Engineering, University of Rochester, Rochester, New York 14627

(Received 7 January 1986; accepted for publication 5 May 1986)

Attenuation measurements can be derived from the decay of backscattered signal with depth in an inhomogeneous material. In cases such as liver tissue, where many small inhomogeneities are likely to be included in sample volumes defined by pulse and beam widths, Rayleigh statistics describe the random nature of the magnitude of backscattered pressure. The statistics of speckle underlie the uncertainties in estimates of attenuation at discrete frequencies, and of the magnitude and frequency dependence of attenuation over a bandwidth. This paper derives expressions for the standard deviations of attenuation magnitude and frequency dependence in terms of parameters such as the dimensions of the region of interest, and the bandwidth of the ultrasonic system. Practical examples are given using published data, and comparisons to other techniques which measure "attenuation slope" are made. The analysis yields insights into trade-offs among variables such as the dimensions and shape of regions of interest, and the segmenting of data in time and frequency domain.

PACS numbers: 43.80.Cs, 43.80.Ev

INTRODUCTION

Ultrasonic attenuation measurements of tissue samples have demonstrated the potential for discriminating normal from diseased tissues. Changes in the attenuation coefficients as a function of time have been documented for a variety of tissues in pathological states. Some examples are dog myocardial tissue following infarction[1] and rat liver tissue during the evolution of carbon tetrachloride damage.[2] The measurement of attenuation *in vivo* using clinical *B*-scan instrumentation has received much attention,[3–8] but the difficulties in this case are generally greater than for laboratory measurements on excised samples. For example, phase-insensitive transmission measurements can be made on isolated samples, but clinical measurements of attenuation must rely on backscattered signals which pass through overlying tissue.

Nonetheless, many time domain and frequency domain strategies exist for attenuation measurements derived from backscattered echoes,[8] and various sources of error complicate the estimation process.[3,9,10] This paper considers only one measurement technique and one source of "error." Specifically, we consider the measurement of the absolute (or true) magnitude of attenuation at independent, discrete frequencies using the decay of ensemble averaged backscattered pressure versus depth. This technique is different from the widely considered class of "attenuation slope" measurements,[5,8] and has the advantages of enabling measurement of the magnitude and frequency dependence of attenuation within a medium, without recourse to *a priori* assumptions concerning the material's frequency dependence of attenuation, the spectral shape of a propagating pulse, and others required for some "attenuation slope" strategies. The source of uncertainty in attenuation estimates considered in this analysis is the underlying random inhomogeneous nature of tissue which results in speckle pattern images. Since the attenuation measurements are based on backscattered echoes, the statistics of speckle directly influence the statistics of, or uncertainty in, the estimation of attenuation. Thus our analysis begins with first-order speckle statistics and we ignore other possible sources of error such as uncompensated beam diffraction effects, quantization errors, and others which may introduce bias or uncertainty.[8–11] The theory is developed from a simple model of weak scattering from randomly positioned inhomogeneities, and results are compared with measurements of speckle statistics and attenuation results from human livers.[4]

An important practical question to be addressed is the minimum volume of tissue required to obtain accurate estimates of the magnitude and frequency dependence of attenuation. This determines possibilities for quantitative tissue characterization in small organs, and the feasibility of true attenuation images with useful resolution.

I. THEORY

In many tissues and phantoms, many small random inhomogeneities (reflectors) are likely to be included in sample volumes interrogated by an ultrasonic pulse, and the backscattered pressure envelope is found to fluctuate in a manner described by Rayleigh statistics.[12–14] On *B*-scan images, this random process results in the speckle patterns commonly seen in tissues such as the liver, and this variability is the root of estimation uncertainties in attenuation measurements.

To demonstrate why the Rayleigh statistics might be observed, we begin with a simple expression for the complex cw backscattered pressure p_{bs} measured at a point located distance r from a sample volume in a nonattenuating medium with small inhomogeneities.

Designating k_0 as the average material wavenumber and $\gamma(\mathbf{r}')$ as the zero-mean fluctuations in impedance as a function of position $\mathbf{r}'$ within the sample volume, it can be shown[3,15] that as a farfield approximation

$$p_{bs}(r) = \frac{A}{r} \int_{v'} e^{j2k_0 \mathbf{n} \cdot \mathbf{r}'} \gamma(\mathbf{r}') dv', \tag{1}$$

where A is a complex factor dependent on frequency, medium density, and amplitude of the incident wave; v' represents the sample volume of integration; and $\mathbf{n}$ is a unit vector pointing in the direction of the incident sound propagation.

A simple argument shows that the magnitude of backscattered pressure, $|p_{bs}|$, is Rayleigh distributed. Within the sample volume v', let the inhomogeneities be K uncorrelated point discontinuities in acoustic impedance. Then,

$$\gamma(\mathbf{r}') = \sum_{i=1}^{K} Z_i \delta(\mathbf{r}' - \mathbf{r}_i), \tag{2}$$

where the magnitudes Z_i have some zero-mean probability density function (pdf). Placing this expression into the backscatter formulation, Eq. (1) becomes

$$p_{bs}(r) = \frac{A}{r} \int_{v'} e^{j2k_0 \mathbf{n} \cdot \mathbf{r}'} \sum_{i=1}^{K} Z_i \delta(\mathbf{r}' - \mathbf{r}_i) dv' \tag{3}$$

$$= \frac{A}{r} \sum_{i=1}^{K} Z_i e^{j2k_0 \mathbf{n} \cdot \mathbf{r}_i}. \tag{4}$$

The last expression reveals that the backscattered pressure is comprised of the sum of independent and identically distributed random variables, where the Z_i are real zero-mean amplitudes, and the exponential terms contribute random phase. Specifically, assuming K is large (>5, say) and applying the central limit theorem, the backscattered pressure must approach a Gaussian, or normal, distribution. Thus the real and imaginary parts of p_{bs} are zero-mean, jointly Gaussian random variables. This immediately determines the pdf for the magnitude of p_{bs} as Rayleigh distributed,[16] where the probability $f_p(p_0)$ that p takes on a particular value p_0 is given by

$$f_p(p_0) = (p_0/a^2)\, e^{-p_0^2/2a^2}, \quad p_0 \geq 0, \tag{5}$$

and the pdf peak occurs at $p_0 = a$. In the backscatter case, the governing parameter a is related to the strength Z_i of the inhomogeneities, and is therefore proportional to the square root of the backscatter coefficient of the material, a quantity itself useful in tissue characterization. A convenient property of the Rayleigh distribution is that the signal-to-noise ratio is independent of the parameter a:

$$\frac{\bar{p}}{\sigma_p} = \left(\frac{\pi/2}{2 - \pi/2}\right)^{1/2} = 1.91. \tag{6}$$

This constant of proportionality is the root of the uncertainties in attenuation estimates, as will be shown below.

In the case of B-scan examination of attenuating tissue separated from the transducer by a nonattenuating water delay line of length r_0, the backscattered pressure from depth d in the tissue can be derived[3] from Eq. (1) as

$$p_{bs}(d) = \frac{A_0}{(r_0 + d)} e^{-2\alpha d} \int_{v'} e^{j2k_0 \mathbf{n} \cdot \mathbf{r}'} \gamma(\mathbf{r}') dv', \tag{7}$$

where α is the pressure attenuation coefficient of the medium. To obtain Eq. (9), it is necessary to assume weak attenuation such that

$$k_0 \gg \alpha, \text{ and } e^{-\alpha r'} \cong 1$$

within the sample volume of integration.[3,15] Using this expression to evaluate the magnitude of backscattered pressure from the ith independent scan line through the tissue, we have

$$|p_{bs}(d)|_i = [A_0 e^{-2\alpha d}/(r_0 + d)]\, p_{i,d}\ , \tag{8}$$

where the backscattered pressure amplitude from the ith waveform and d th depth segment in the absence of attenuation $p_{i,d}$ are independent, identically distributed Rayleigh random variables, assuming uniform transmission into the medium, use of nonoverlapping depth segments, and stationary scattering statistics. Thus the problem reduces to the estimation of the unknown exponential decay in the presence of the "noisy" coefficients. The pressure magnitudes can be written in terms of their mean and a random term,

$$p_{i,d} = \bar{p} \pm \epsilon_{i,d} = \bar{p}(1 \pm \epsilon_{id}/\bar{p}), \tag{9}$$

where $E\{\epsilon\} = 0$, and by virtue of the Rayleigh distribution and Eq. (6),

$$\sigma_\epsilon/\bar{p} = 0.524. \tag{10}$$

An improved signal-to-noise ratio is obtained by averaging results of N independent scan lines through the tissue,

$$\hat{p}(d) = \hat{p}_d\, e^{-2\alpha d}, \tag{11}$$

where

$$\hat{p}_d = \frac{1}{N} \sum_{i=1}^{N} p_{i,d}\ . \tag{12}$$

Assuming large N (>5, for example) and again invoking the central limit theorem, the mean pressure magnitude from depth d, $\hat{p}_d$, is approximated as normal or Gaussian distributed random variable and can also be written in terms of a mean value and fluctuating term,

$$\hat{p}_d = \bar{p}(1 \pm \hat{\epsilon}/\bar{p}), \tag{13}$$

where

$$\sigma_{\hat{\epsilon}}/\bar{p} = 0.524/\sqrt{N}\ . \tag{14}$$

The exponential decay of $\hat{p}(d)$ is then used to estimate attenuation. The natural log of Eq. (11) yields a linear relation (now using x as the depth variable):

$$\ln[\hat{p}(x)] = -2\alpha x + \ln[\hat{p}_x] \tag{15}$$

or

$$y = bx + a\ . \tag{16}$$

The error in estimating $b(=-2\alpha)$ is directly related to the variation in $\ln[\hat{p}_x]$. A simplification of the log transformed variable results if we write using Eqs. (16) and (13):

$$a = \ln[\hat{p}_x] = \ln[\bar{p}(1 \pm \hat{\epsilon}/\bar{p})]. \tag{17}$$

Using the approximation

$$\ln[1 + z] \cong z \quad \text{for} \quad z \ll 1, \tag{18}$$

then from the last two expressions

$$a \cong \ln \bar{p} \pm \hat{\epsilon}/\bar{p}\ . \tag{19}$$

Using the result with Eq. (14) yields

$$\sigma_y = \sigma_a = 0.524/\sqrt{N}\ . \tag{20}$$

The last expression bears examination. First, the parameter N, which is the number of independent scan lines averaged, is required to be large in order to validate the use of the small

noise-to-signal log expansion, enabling continued use of analysis based on normally distributed variables. Furthermore, the last expression shows that the variability in backscattered pressure, originally proportional to the mean backscattered pressure, is transformed to a constant in the log variable domain. This concept is illustrated in Fig. 1(a) and (b).

The variance of a least-squares estimate for the slope b can now be written as[17,18]

$$\sigma_b^2 = \frac{\sigma_y^2}{[\Sigma_{j=1}^{M}(X_j - \overline{X})^2]}, \tag{21}$$

where there are M independent sample volume depths for which data are obtained. Assuming the sample volumes are successively deeper in the medium and are separated by uniform distance ΔX, then an empirically derived substitution, valid for $M \leqslant 30$, is

$$\sum_{j=1}^{M}(X_j - \overline{X})^2 \cong 2\Delta X^2\left(\frac{M-1}{2}\right)^{5/2}, \tag{22}$$

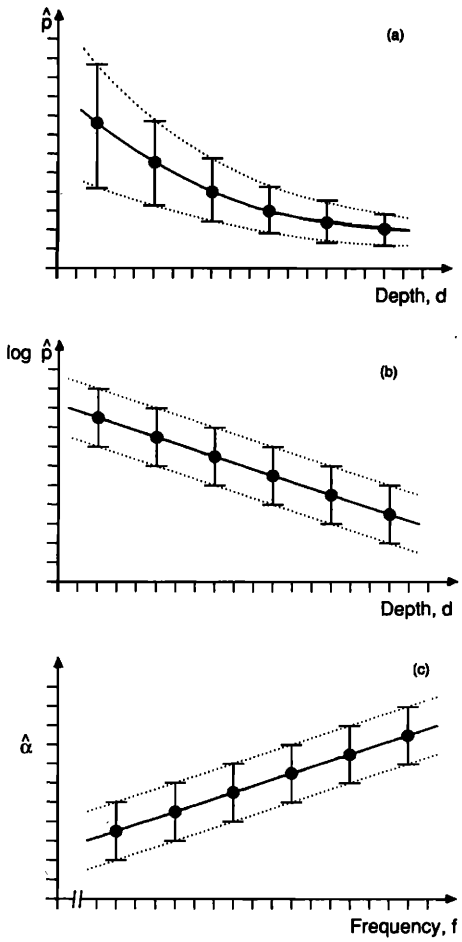

FIG. 1. The propagation of uncertainties. Solid lines are expected values; error bars represent standard deviations of sampled values. Average backscattered pressure versus depth is shown in (a). The standard deviations are proportional to mean values as a result of underlying Rayleigh statistics, but are minimized by averaging over independent scan lines through a medium. Thus in (b) the error bars of the log transformed variables will be symmetric and constant. Resulting attenuation estimates at discrete frequencies, shown in (c), will have a constant standard deviation which is related to the underlying Rayleigh statistics and size of the region of interest employed. As frequency increases, the magnitude of attenuation increases, and thus the fractional errors decrease.

which depends only on the number of sample depths and their spacing, not their absolute location within the medium.

Combining Eqs. (22), (21), and (20) produces the desired result:

$$\sigma_\alpha = \frac{0.44}{\Delta X(N^{1/2})\ (M-1)^{5/4}}, \tag{23}$$

which shows that the expected variability or error in attenuation measurement is a constant which depends on the number and spacing of the sample volumes, not on the material backscatter coefficient (the mean value a of the Rayleigh statistics) or the magnitude of attenuation. Thus the fractional error in attenuation σ_α/α decreases with increasing frequency, as shown in Fig. 1(c).

When the value of attenuation is measured at F independent discrete frequencies separated by Δf MHz increments, then the frequency dependence of attenuation may be determined. Using a power law assumption, the attenuation estimates $\alpha(f)$ may be fit:

$$\alpha(f) = \alpha_0 f^n, \tag{24}$$

where α_0 and n characterize the magnitude of attenuation (at 1 MHz given f in MHz) and the frequency dependence, respectively. Again, a log transformation can be employed to derive a least-square error fit:

$$\ln[\alpha(f)] = \ln\alpha_0 + n\ln[f] \tag{25}$$

or

$$y' = a' + b'x'. \tag{26}$$

From the previous analysis, the variability in the attenuation estimates $\alpha(f)$ is a known constant. Therefore, the variance of the least-squares estimates of a' and b' ($\ln\alpha_0$ and n) can be determined given the following assumptions. The attenuation estimates are written in terms of a correct value $\hat{\alpha}(f)$ plus a noise term,

$$\alpha(f) = \hat{\alpha}(f) + \epsilon' = \hat{\alpha}(f)[1 + \epsilon'/\hat{\alpha}(f)], \tag{27}$$

where $\sigma_{\epsilon'}$ is identical to σ_α and is given by Eq. (23). Given a small fractional error of the attenuation estimate,

$$\frac{|\epsilon'|}{\hat{\alpha}(f)} \ll 1 \quad \text{or} \quad \frac{\sigma_\alpha}{\hat{\alpha}(f)} \ll 1, \tag{28}$$

then applying the log approximation of Eq. (18), the transformed attenuation estimate can be rewritten as

$$y' = \ln[\alpha(f)] \cong \ln\hat{\alpha}(f) + \epsilon'/\hat{\alpha}(f). \tag{29}$$

Thus

$$\sigma_{y'} = \sigma_\alpha/\hat{\alpha}(f). \tag{30}$$

The standard deviation of y' is equal to the fractional error of the attenuation estimate and is not constant over any finite bandwidth, nor is it simply proportional to the expected value of the data. However, simplified expressions which can be generalized in closed form can only be written for the case of constant error. Thus we assume that the data are obtained over a finite bandwidth for which a representative constant value of $\sigma_{y'}$ may be obtained:

$$\sigma_{y'} = \sigma_\alpha/\hat{\overline{\alpha}}, \tag{31}$$

where $\hat{\overline{\alpha}}$ is some average value of attenuation coefficient within the bandwidth of interest. Given this coarse but use-

ful approximation we have from least-squares error analysis[17,18]

$$\sigma_{a'}^2 = \sigma_{y'}^2 \left\{ \frac{\Sigma \ln^2(f_i)}{F\Sigma\left[\ln(f_i) - \overline{\ln(f)}\right]^2} \right\}, \tag{32}$$

where the summation is over discrete frequencies $i = 1$ to F. Using the small error approximation of Eq. (18) to revert from the log transformed variable a' to the parameter of interest α_0 we find that the fractional error in estimating the magnitude is given by

$$\frac{\sigma_{\alpha_0}}{\alpha_0} = \sigma_{a'} = \frac{\sigma_a}{\hat{\bar{\alpha}}} \left\{ \frac{\Sigma \ln^2(f_i)}{F\Sigma\left[\ln(f_i) - \overline{\ln(f)}\right]^2} \right\}^{1/2}. \tag{33}$$

If an estimation is made of the magnitude of attenuation $\hat{\bar{\alpha}}$ at some frequency $\bar{f}$ near the center of the bandwidth, then by an axis shift to $\overline{\ln(f)} = 0$, the sum of squares terms in Eq. (33) approaches unity, and the uncertainty reduces to

$$\sigma_{\hat{\bar{\alpha}}} = \sigma_\alpha / \sqrt{F}, \tag{34}$$

which is merely the fractional error in any single estimate of attenuation, divided by the square root of the number of independent frequencies for which estimates were obtained.

The last parameter to be examined is the frequency dependence, or slope n. From Bevington,[18] the standard deviation in this estimate is

$$\sigma_n = \sigma_{y'} / \sqrt{\Sigma\left[\ln(f_i) - \overline{\ln(f)}\right]^2}. \tag{35}$$

Since the discrete frequencies f_i are, in general, equally spaced, the log variables will have unequal spacing:

$$\begin{aligned} \Delta \ln(f_i) &= \ln(f_i + \Delta f) - \ln(f_i) \\ &= \ln(1 + \Delta f / f_i) \cong \Delta f / f_i, \end{aligned} \tag{36}$$

in the last step assuming $\Delta f / f \ll 1$. We further assume that the log frequency increment can be represented over a finite bandwidth by some mean quantity $\Delta f / \bar{f}$. Then Eq. (35) becomes, using Eq. (22):

$$\sigma_n = \frac{1.68}{(F-1)^{5/4}} \frac{\bar{f}}{\Delta f} \sigma_{y'} = \frac{1.68\, \bar{f} \sigma_\alpha}{(F-1)^{5/4} \Delta f \bar{\alpha}}. \tag{37}$$

The significance of these expressions is discussed in the following section.

II. RESULTS AND DISCUSSION

A. The acoustic model

A number of simplifications were made in arguments for underlying Rayleigh statistics. Scatterers were assumed to be small, weak, and randomly distributed in space and impedance. In practice, Rayleigh statistics are often noted in speckle image regions of tissue or phantoms.[12–14] Figure 2 shows a histogram of magnitude of backscattered pressure at 2.58 MHz obtained from the Fourier transform of time-gated echoes received at constant depth from 100 scan lines laterally spaced by 0.4 mm in an adult human liver. Each sample volume was 0.75 cm in depth and 0.4 cm transverse, based on the data windowing and beamwidth, respectively. The data are compared with a theoretical Rayleigh distribution which is scaled to the mean of the experimental data. These measurements, and all others presented in this section, were obtained from an Octoson B-scan instrument[19]

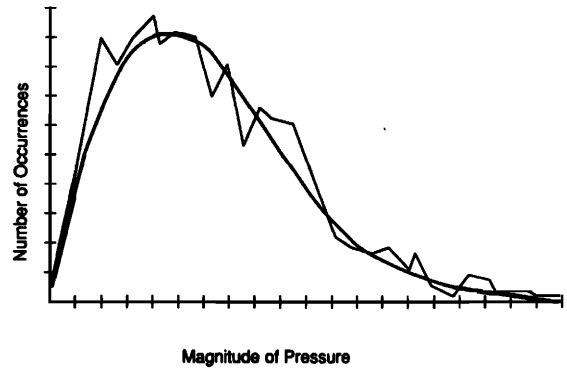

FIG. 2. A histogram of the magnitude of backscattered pressure at 2.5 MHz, obtained from over 100 sample volumes in a speckle region of normal liver. Smooth line is a Rayleigh distribution which was scaled the mean of the experimental data.

(2.5-MHz center frequency, 1-MHz usable bandwidth) using signal processing described previously.[3,4] The magnitude of backscattered pressure from liver, obtained using this system, consistently yielded Rayleigh first-order statistics similar to those shown in Fig. 2, when care was taken to eliminate sample volumes which included obvious deviations from the model, such as specular reflections from larger vessels or liver boundaries. Other first-order statistics such as a Rician pdf may be found under special conditions.[14] In the particular case of Rician statistics, the signal-to-noise ratio increases, compared to the Rayleigh case, and therefore the estimation precision would improve proportionally, assuming stationary statistics within the region of interest.

B. Parameter uncertainties

The expression for the standard deviations in estimates of attenuation at any single frequency α and then the power law parameters α_0 and n over a bandwidth deserve additional comment.

First, the uncertainty in estimating attenuation given by Eq. (23) has the intuitively reasonable result: The variability is proportional to a constant which is directly related to the underlying speckle statistics, and can be reduced as a function of the number M and spacing of ΔX independent sample volumes along the axis of insonation, and also the number N of independent scan lines which are averaged. The difference in powers of N and M demonstrate the relative importance of data along the axis of insonation. Put another way, Eq. (23) demonstrates that estimates of attenuation from isovolumetric regions will not, in general, yield equal results. In Fig. 3(a) and (b), two regions are shown with equal volume, $v = (M\Delta x)(N\Delta y)(\Delta z)$, where Δz is assumed to be on the order of a beamwidth, and Δy a half beamwidth, the minimum distance required to ensure independent scan lines.[12,13] In Fig. 3(a), $M = 10$ and $N = 5$, but in Fig. 3(b), $M = 5$ and $N = 10$. Using Eq. (23), the ratio of s.d. of attenuation measurements will be

$$\frac{\sigma_{\alpha v_1}}{\sigma_{\alpha v_2}} = \frac{(10)^{1/2}(5)^{5/4}}{(5)^{1/2}(10)^{5/4}} \cong 0.6. \tag{38}$$

This demonstrates the relative advantages of adding increased depth segments as opposed to lateral averaging.

As a practical example of measurement uncertainty, we

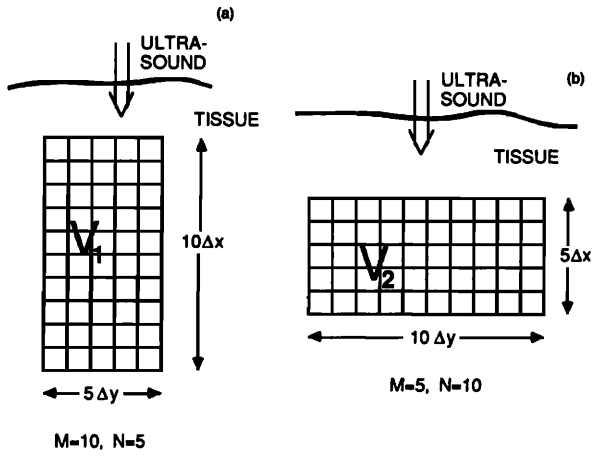

FIG. 3. Isovolumetric regions of interest segmented into independent scan lines (Δy = one-half beamwidth), and depth segments (Δx = axial length chosen by proper windowing of digitized rf echo). In (a), greater depth information is available, whereas in Fig. 5(b), increased lateral averaging is available. The uncertainty in estimation of attenuation at any frequency is lower by 60% in case 5(a) compared to 5(b) because a least-squares error estimation strongly favors the added depth information.

consider the early results of liver attenuation obtained from the Rochester system,[3,4] where an approximate 4-×5-cm region of tissue was analyzed. In this case, time domain Blackman windows were spaced with a distance of $\Delta X = 0.375$ cm; there were $M = 14$ independent depths and $N = 12$ independent scan lines per region of interest. Thus from Eq. (23) the s.d. of the measurements was

$$\sigma_\alpha = \frac{(0.44)}{(0.375)(12)^{1/2}(13)^{5/4}} = 0.014 \text{ Np/cm}. \quad (39)$$

Using a typical value of $\alpha = 0.15$ Np/cm for 3 MHz,[4] the fractional error for these measurements expressed in percent is

$$\sigma_\alpha/\alpha_{3\text{MHz}} \cong \pm 9\%. \quad (40)$$

Thus, with this system operating in a frequency band of 2–3 MHz, an approximately 4-×5-cm region was required to obtain less than 10% fractional error on any single measurement of attenuation.

In deriving the magnitude and frequency dependence of attenuation over a bandwidth, the standard deviations in α_0 and n were linked directly to the uncertainty in attenuation at any individual frequency σ_α. Also, the standard deviation in estimate of attenuation $\hat{\bar{\alpha}}$ near the center frequency is shown by Eq. (34) to be less than σ_α by a factor of $1/\sqrt{F}$, where F is the number of discrete, independent frequencies at which attenuation estimates were obtained. The correct interpretation is that $\hat{\bar{\alpha}}$ is merely the group average of F attenuation estimates over the bandwidth. If the bandwidth does not include 1 MHz, then the value of α_0 is a projection out of the range of data, and Eq. (33) is used. Again, referring to the Rochester system,[3,4] attenuation estimates were obtained at $F = 15$ discrete frequencies between 2 and 3 MHz. Assuming a 10% average fractional error for individual attenuation estimates, then using Eq. (34),

$$\sigma_{\hat{\bar{\alpha}}}/\hat{\bar{\alpha}} = 10\%/\sqrt{15} = 2.6\% \quad \text{at} \quad 2.5 \text{ MHz}. \quad (41)$$

Whereas projecting to 1 MHz to find α_0, using Eq. (33),

$$\frac{\sigma_{\alpha_0}}{\alpha_0} = \frac{10\%}{\sqrt{F}}\left(\frac{\Sigma \ln^2(f_i)}{\Sigma[\ln(f_i) - \overline{\ln(f)}]^2}\right) = 17\%, \quad (42)$$

a larger error than obtained for the 2.5-MHz group estimate.

Turning to the estimation of the frequency dependence n, Eq. (37) shows that the s.d. is proportional to the fractional error in attenuation measurements, and inversely proportional to the number of and spacing between frequency points. For the Rochester data,[3,4] with $\bar{f} \cong 2.5$ MHz, $\Delta f = 5/64$ MHz, and using a single scan with fractional error of attenuation estimates of 10%, then Eq. (37) yields

$$\sigma_n = \frac{1.68(2.5)(64)10\%}{(14)^{5/4}(5)} \cong 20\%. \quad (43)$$

For the clinical data reported by Parker *et al.*,[4] at least two parallel scans separated by 10 mm were used for final estimates of α_0 and n, thereby reducing the per-scan uncertainties reported above by an additional factor of at least $1/\sqrt{2}$.

C. Relation between estimates of α_0 and n

In practice, the estimated values of α_0 and n do not distribute evenly or normally about the correct values for any given tissue or phantom. Instead, the values of α_0 and n estimated from small regions of interest tend to take on a quasi-reciprocal relation whereby if the estimate of α_0 is above the correct value, then the estimate for n tends to be low, such that the result yields an accurate magnitude of attenuation at the mean frequency (or more accurately, the mean log frequency, although for small bandwidths the distinction is not great). Understanding of this phenomenon is crucial in interpreting results. The effect can be explained with the aid of Fig. 4, where a log–log plot of attenuation versus frequency is shown for an attenuating medium which may be characterized by the two power law parameters α_0 and n. We then assume that attenuation estimates are obtained over a bandwidth of $f_2 - f_1$ MHz. Error bars are drawn to represent the uncertainty σ_α at f_1 and f_2, whereas the smaller error at mean frequency represents the more accurate group average estimate of attenuation at the mean frequency, given by Eq. (34). (The smaller error bar can alternatively be thought of as a constraint that the power law fit will be unbiased at the center frequency.) There exists a family of curves which lie within all error bars. Thus $\ln \alpha_0$ (the intercept) and n (the slope) are seen on the dotted lines of Fig. 4 to vary inversely.

To quantify this effect, the slope and intercept can be found for the two dotted lines of Fig. 4 which represent the extreme members of the family of lines lying within all error bars. The high and low intercept lines, labeled lines 1 and 2, respectively, pass through the log of the points:

$$\begin{aligned} &1: \quad (\alpha_1 + \sigma_\alpha, f_1); \ (\alpha_2 - \sigma_\alpha, f_2), \\ &2: \quad (\alpha_1 - \sigma_\alpha, f_1); \ (\alpha_2 + \sigma_\alpha, f_2). \end{aligned} \quad (44)$$

Taking the log transform of these points, and applying the small error approximation to separate error terms from the log variables, the slope b and intercept a can be obtained for line 1:

$$b_1 = n - 2\epsilon_\alpha/\ln(f_2/f_1), \quad (45)$$

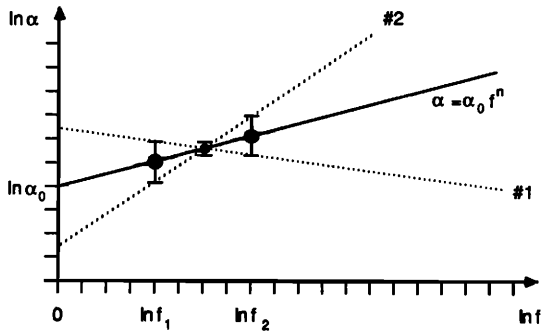

FIG. 4. A power law fit of attenuation versus frequency, using log variables. If attenuation estimates are available at discrete frequencies between f_1 and f_2, then estimates of the power law parameters are most likely to fall within the "bow tie" region shown between lines #1 and #2, centered about the correct values of α_0 and n which describe the attenuating medium.

$$a_1 = \ln(\alpha_0) + \epsilon_\alpha \frac{\ln(f_2 \cdot f_1)}{\ln(f_2/f_1)}, \tag{46}$$

where $\epsilon_\alpha = \sigma_\alpha / \bar{\alpha}$, some average fractional error of individual attenuation estimates. For line 2, the signs on the error terms of Eqs. (45) and (46) are reversed.

As a practical example, let $\alpha_0 = 0.05$ Np/cm-MHz and $n = 1$ represent values for normal liver.[4] Furthermore, let $f_1 = 2$ MHz, $f_2 = 3$ MHz, and $\sigma_\alpha/\alpha = 0.03$. Then the extreme estimates of a power law fit are either:

$$\alpha_{0_1} = 0.044; \quad n_1 = 1.15,$$

or

$$\alpha_{0_2} = 0.057; \quad n_2 = 0.85.$$

Despite the apparent difference between these sets of values, both yield the same magnitude of attenuation, 0.126 Np/cm, near the center frequency 2.5 MHz. These parameter values plotted on α_0 vs n space are shown in Fig. 5. Extreme values are also shown for other fractional errors, and the result demonstrates that estimated values of α_0 and n, which yield identical attenuation magnitudes near the mean frequency, tend to cluster along a reciprocal or hyperbolic shaped curve. Thus, when comparing attenuation results from different individuals, a strong claim for differentiation of results can be made only when estimates fall on mutually exclusive reciprocal curves in α_0 vs n space.

Figure 6 depicts the scatter of estimates of α_0 and n obtained from independent regions of interest within two human livers. The values are seen to cluster around the locus of points which yield constant attenuation at 2.5 MHz.

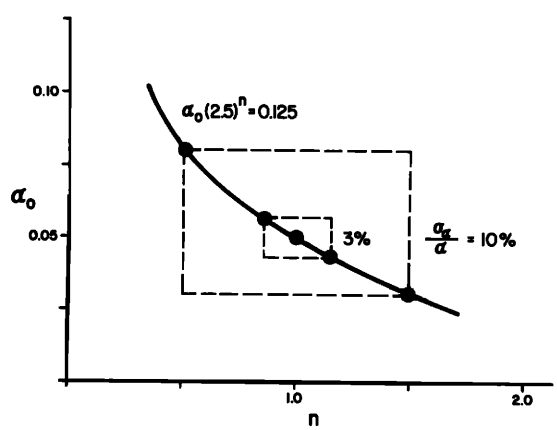

FIG. 5. Errors in estimations of power law parameters α_0 and n are linked in a quasireciprocal relationship. Uncertainties in these parameters can be drawn in α_0 versus n space as a locus of points which yield the same value of attenuation at the center frequency; $\alpha_0(\bar{f})^n$ = constant. (This is in contrast to the common representation of independent uncertainties of two variables, which would typically be drawn as a point with both horizontal and vertical error bars drawn.) As the standard deviation of the individual attenuation estimates increases, the spread of power law estimates increases.

D. Strategies to minimize volume requirements

The system discussed in Sec. II B obtained 10% fractional error for individual attenuation estimates and close to 20% for the group estimate of power law parameters, utilizing a 4-×5-cm region of tissue and 1-MHz bandwidth. This region of interest is too large for application to focal diseases or small tumors, or for use on smaller organs such as the kidney, which would require further subdivision of medulla and cortex echoes in order to maintain the stationary backscatter statistics required for attenuation analysis.

If attenuation imaging is to be based on a single parameter, then the most accurate is the group estimate of attenuation $\hat{\bar{\alpha}}$ at the center frequency, obtained by either evaluating the power law fit at the center frequency, or equivalently taking the mean of the log transformed individual estimates of attenuation. The standard deviation of this parameter is from Eqs. (23) and (34),

$$\sigma_{\hat{\bar{\alpha}}} = \frac{0.44}{(\Delta X)(M-1)^{5/4}(N \cdot F)^{1/2}}. \tag{47}$$

Assuming a tissue dimension of L cm is available along the axis of insonation, with a system bandwidth of B Hz, the problem is to segment echoes optimally into sample volumes, given that resolution in the frequency domain is inversely proportional to resolution in the time domain. Assuming a time domain window of $\Delta t = 2\Delta X / C$, where $C/2$ is the round-trip speed of sound in the medium, then the resolution in the frequency domain Δf is given by the inverse of the time window:

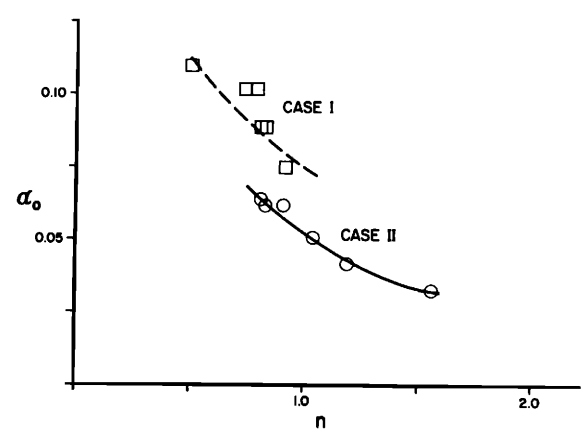

FIG. 6. The scatter of pairs of (α_0, n) estimates obtained from multiple independent regions of interest within the livers of two individuals. The power law estimates tend to fall on the locus of (α_0, n) points which yield a constant value of attenuation at 2.5 MHz, the center frequency of the system used to collect data.

$$\Delta f \cong 1/\Delta t = C/2\Delta X. \quad (48)$$

Segmenting the available length L and bandwidth B, we have the relations:

$$\Delta X = L/M \quad \text{and} \quad \Delta f = B/F. \quad (49)$$

Substituting these into the error expression of Eq. (47) to eliminate ΔX and F yields:

$$\sigma_{\hat{\bar{\alpha}}} = \frac{0.44(C/2)^{1/2}}{L^{3/2}N^{1/2}B^{1/2}[(M-1)^{5/4}/M^{3/2}]}. \quad (50)$$

In the above expression, the term in square brackets is insensitive to variations in M. Conveniently, the quantity $(M-1)^{5/4}/M^{3/2}$ is very close to 0.44 over a range of $3 \leqslant M \leqslant 30$. This implies that the least-squares error estimate of attenuation depends strongly on the overall dimensions of the medium and the bandwidth employed, but is nearly independent of how the time (sample volume depth) and frequency domains are segmented.

Substituting the constant 0.44 for the function of M in square brackets of Eq. (50) produces the desired result:

$$\sigma_{\hat{\bar{\alpha}}} = \left(\frac{C/2}{L^3 \cdot N \cdot B}\right)^{1/2}. \quad (51)$$

To illustrate this result, let us calculate the error bounds on $\hat{\bar{\alpha}}$ using data from a 1-$\times$1-cm region of tissue. Assume the use of a hypothetical 6.3-MHz bandwidth, 6.3-MHz center frequency, $f/10$, scanning instrument. (For comparison purposes, these are the same system parameters employed by Kuc in calculations of the variance in measurement of attenuation slope.[20]) The diffraction limited beamwidth near the focus will be approximately 2.8 mm, thus using half-beamwidth overlap; $N = 7$ independent scan lines may be obtained within the 1-cm lateral dimension. Given $C/2 = 750$ m/s, Eq. (51) yields:

$$\sigma_{\hat{\bar{\alpha}}} = \left(\frac{(0.75\times 10^5)}{1^3 \cdot 7 \cdot 6.3\times 10^6}\right)^{1/2} = 0.04 \text{ Np/cm}. \quad (52)$$

This produces an 11% fractional error in attenuation at the center frequency, using a normal liver value of attenuation equal to 0.38 Np/cm, at 6.3 MHz. This result is significant since it demonstrates that attenuation maps or images of 1-cm^2 resolution, with approximately 10% accuracy, could be obtained using a 6.3-MHz B-scan system. If compound scanning is possible (as is routinely the case in abdominal imaging using the Octoson), then either the dimensions or the error bounds can be further reduced.

In contrast, Kuc applies the same system parameters to the estimate of attenuation slope β. For the 6.3-MHz, $f/10$ case, a 1-cm^2 region of interest yields a standard deviation in β of 0.1 dB/cm-MHz, using either the log spectral difference or Gaussian spectral shift approaches.[20] Comparisons between these approaches and those outlined in this paper and others[3,4] can only be made for the special case of a medium where attenuation increases linearly with frequency. Under these conditions:

$$\alpha = \beta f \quad \text{and} \quad \sigma_\alpha = \sigma_\beta \cdot f. \quad (53)$$

Converting the units of β gives

$$\sigma_\beta = 0.1 \text{ dB/cm-MHz} = 0.0115 \text{ Np/cm-MHz}, \quad (54)$$

whereas our group estimate at the center frequency, using the results of Eq. (52), yields:

$$\sigma_{\hat{\bar{\alpha}}}/6.3 \text{ MHz} = 0.0063 \text{ Np/cm-MHz}, \quad (55)$$

or a 55% drop in error bounds as compared to the β estimators.

The improved precision in our approach may be attributable to the fact that the β estimators are applied as pairwise comparisons of signals from different depths, whereas our approach uses all depth information for least-squares error curve fit. The latter approach is a more efficient use of data.

III. CONCLUSION

The magnitude of attenuation may be estimated at discrete, independent frequencies by measuring the decay of ensemble averaged backscatter pressure magnitude as a function of depth. The fluctuation introduced by random, multiple, small scatterers is well described by Rayleigh statistics, which form the basis for calculations of uncertainties in estimates of the magnitude and frequency dependence of attenuation within a region of interest. A number of important concepts emerge from the analysis.

(1) Square regions of interest are not the optimal shape for measuring attenuation. The least-squares estimation process reveals that parameter uncertainties are reduced more by extending depth or range than by increasing lateral averaging.

(2) Assuming the attenuation coefficients obtained over a finite bandwidth can be well described by a power law fit, then each tissue or region of interest can be characterized by two parameters, the magnitude α_0 and frequency dependence n of attenuation. Alternatively, a single parameter can be derived from the power law fit, the magnitude of attenuation at the center frequency $\hat{\bar{\alpha}}$. This group estimate is more precise than either the estimates of α_0 and n, or any single estimate of attenuation at a discrete frequency within the bandwidth.

(3) Two-parameter classification of tissue by α_0 and n may be useful in detecting specific changes in tissue; however, the errors in α_0 and n involve a quasireciprocal relation. Estimates of α_0 and n from different regions of interest within the same medium will tend to cluster on a curve of constant attenuation at the center frequency. Claims for differentiation of tissue types can be made only when the estimates lie on mutually exclusive curves in α_0 vs n space.

(4) The 1-cm^2 region of interest will permit estimates of $\hat{\bar{\alpha}}$, with approximately 10% error, given a 6.3-MHz (center frequency and bandwidth), $f/10$ ultrasonic imaging system. The use of alternative methods for estimating attenuation slope produces nearly twice the uncertainty given the same system parameters. Attenuation imaging of smaller regions of interest will require the use of increased bandwidths and/or compound scanning.

ACKNOWLEDGMENTS

Thanks are extended to Professor R. C. Waag and J. A. Campbell for their helpful comments and suggestions. This work was supported by the Whitaker Foundation, the Diagnostic Ultrasound Research Laboratory Industrial Associates, NIH Grant CA39516, and NSF Grant ECS8414315.

[1]M. O'Donnell, J. W. Mimbs, and J. G. Miller, "The relationship between collagen and ultrasonic attenuation in myocardial tissue," J. Acoust. Soc. Am. **65**, 512–517 (1979).
[2]K. J. Parker and T. A. Tuthill, "CCl_4 induced changes in ultrasonic properties of liver," IEEE Trans. Biomed. Eng. **BME-33**, 453–460 (1986).
[3]K. J, Parker and R. C. Waag, "Measurement of attenuation within regions selected from *B*-scan images," IEEE Trans. Biomed. Eng. **BME-30**, 431–437 (1983).
[4]K. J. Parker, R. M. Lerner, and R. C. Waag, "Attenuation of ultrasound: Magnitude and frequency dependence for tissue characterization," Radiology **153**, 785–788 (1984).
[5]R. Kuc and M. Schwartz, "Estimating the acoustic attenuation coefficient slope for liver from reflected ultrasound signals," IEEE Trans. Sonics Ultrason. **SU-26**, 353–362 (1979).
[6]N. Maklad, J. Ophir, and V. Balsara, "Attenuation of ultrasound in normal liver and diffuse liver disease *in vivo*," Ultrason. Imaging **6**, 117–125 (1984).
[7]F. L. Lizzi and D. J. Coleman, "Ultrasonic spectrum analysis in ophthalmology," in *Recent Advances in Ultrasound in Biomedicine*, edited by D. N. White (Research Studies Press, 1977).
[8]S. Leeman, L. Ferrari, J. P. Jones, and M. Fink, "Perspectives on attenuation estimation from pulse-echo signals," IEEE Trans. Sonics Ultrason. **SU-31** (4), 352–361 (1984).
[9]P. A. Naryana and J. Ophir, "On the validity of the linear approximation in the parametric measurement of attenuation in tissues," Ultrason. Med. Biol. **9**, 357–361 (1983).
[10]M. A. Fink and J. F. Cardoso, "Diffraction effects in pulse-echo measurements," IEEE Trans. Sonics Ultrason. **SU-31**, 313–329 (1984).
[11]R. Kuc, "Estimating reflected ultrasound spectra from quantized signals," IEEE Trans. Biomed. Eng. **BME-32**, 105–111 (1985).
[12]C. B. Burckhardt, "Speckle in ultrasonic *B*-mode scans," IEEE Trans. Sonics Ultrason. **SU-25**, 1–6 (1978).
[13]J. G. Abbott and F. L. Thurstone, "Acoustic speckle, theory and experimental analysis," Ultrason. Imaging **1**, 303–324 (1979).
[14]R. Wagner and S. Smith, "Statistics of speckle in ultrasound *B*-scans," IEEE Trans. Sonics Ultrason. **30**, 156–163 (1983).
[15]R. C. Waag, R. M. Lerner, P. P. K. Lee, and R. Gramiak, "Ultrasonic diffraction characterization of tissue," in *Ultrasound in Biomedicine, Vol. I, Tissue Characterization and New Imaging Techniques*, edited by D. N. White (Research Studies, Forest Grove, OR, 1978), pp. 87–116.
[16]A. Papoulis, *Probability, Random Variables, and Stochastic Processes* (McGraw-Hill, New York, 1984), 2nd ed., Chap. 6.
[17]N. Draper and H. Smith, *Applied Regression Analysis* (Wiley, New York, 1967), Chap. 1.
[18]P. R. Bevington, *Data Reduction and Error Analysis for the Physical Sciences* (McGraw-Hill, New York, 1969), Chap. 6.
[19]Ausonics Corp., 2915 South 160th Street, New Berlin, WI 53151.
[20]R. Kuc, "Bounds on estimating the acoustic attenuation of small tissue regions from reflected ultrasound," Proc. IEEE **73**, 1059–1168 (1985).